Referenceless Perceptual Fog Density Prediction Model

Lark Kwon Choi*[a], Jaehee You[b], and Alan C. Bovik[a]

[a]Laboratory for Image and Video Engineering (LIVE), Department of Electrical and Computer Engineering, The University of Texas at Austin, Austin, TX, USA
[b]Department of Electronic and Electrical Engineering, Hongik University, Seoul, Korea

ABSTRACT

We propose a perceptual fog density prediction model based on natural scene statistics (NSS) and "fog aware" statistical features, which can predict the visibility in a foggy scene from a single image without reference to a corresponding fogless image, without side geographical camera information, without training on human-rated judgments, and without dependency on salient objects such as lane markings or traffic signs. The proposed fog density predictor only makes use of measurable deviations from statistical regularities observed in natural foggy and fog-free images. A fog aware collection of statistical features is derived from a corpus of foggy and fog-free images by using a space domain NSS model and observed characteristics of foggy images such as low contrast, faint color, and shifted intensity. The proposed model not only predicts perceptual fog density for the entire image but also provides a local fog density index for each patch. The predicted fog density of the model correlates well with the measured visibility in a foggy scene as measured by judgments taken in a human subjective study on a large foggy image database. As one application, the proposed model accurately evaluates the performance of defog algorithms designed to enhance the visibility of foggy images.

Keywords: Fog, fog density, fog visibility, fog aware, defog algorithm assessment, natural scene statistics

1. INTRODUCTION

The perception of outdoor natural scenes is important for understanding the environment and for executing visual activities such as object detection, recognition, and navigation. In bad weather, visibility can be seriously degraded due to the absorption or scattering of light by atmospheric particles such as fog, haze, and mist.[1] Since the reduction of visibility can dramatically degrade an operator's judgment in a vehicle and induce erroneous sensing in remote surveillance systems, visibility prediction and enhancement methods on foggy images have been widely studied.[2-13]

Visibility prediction algorithms on a foggy image require a corresponding fogless image of the same scene under different weather conditions to compare visibility[2] or salient objects in a foggy image such as lane markings or traffic signs to supply distance cues[3]. Hautiere *et al.*'s automatic fog detection and estimation of visibility distance method[4] depends on side geographical information obtained from an onboard camera, so such methods work only under limited conditions and are not necessarily applicable to general foggy scenes. Regarding visibility enhancement of foggy images, diverse defog algorithms[5-13] have been introduced. Since direct visibility prediction from a foggy image is difficult, most defog algorithms use the estimated depth or transmission map to improve visibility using assumptions from, e.g., Koschmieder's atmospheric scattering model[14]. In addition, early on, the performance of defog algorithms was only evaluated subjectively due to the absence of any appropriate visibility assessment tool. Recently, gain parameters[11] were compared before and after a defog algorithm, or modified image quality assessment (IQA) tools were applied[9]. However, the subjective evaluation approach is not useful for large remote or mobile data, the gain comparison method requires both the original foggy image and the corresponding defogged image, and IQA methods are generally inappropriate since they are designed to measure distortion levels rather than the visibility of a foggy image.

In this paper, we propose, for the first time (to our knowledge), a perceptual fog density prediction model. This model can predict the visibility in a foggy scene without reference to a corresponding fogless image, without side camera information, without training on human-rated judgments, and without dependency on salient objects in a foggy image. The proposed fog density predictor only makes use of measurable deviations from statistical regularities observed in natural foggy and fog-free images. The "fog aware" statistical features that define the perceptual fog density are derived from a corpus of 160 natural foggy and fog-free images based on a space domain regular natural scene statistic (NSS)[15,16]

Human Vision and Electronic Imaging XIX, edited by Bernice E. Rogowitz, Thrasyvoulos N. Pappas, Huib de Ridder, Proc. of SPIE-IS&T Electronic Imaging, Proc. of SPIE Vol. 9014, 90140H
 · doi: 10.1117/12.2036477

model and observed characteristics of foggy images including low contrast, faint color, and shifted intensity. The spatial NSS model involves computing local mean subtracted contrast normalized coefficients (MSCN)[16]. The MSCN and the pairwise product of neighboring MSCN coefficients along vertical orientations serve as fog aware features. Other fog aware statistical features are derived from the local mean and local coefficient of variance for sharpness[17], the contrast using edge energy[18], the image entropy[19], the pixel-wise dark channel prior[9], the color saturation, and the colorfulness[20].

A total of 9 local fog aware statistical features are computed for each $P \times P$ partitioned image patch. Then, a multivariate Gaussian (MVG)[21] distribution is applied to predict the fog density of a test foggy image by using a Mahalanobis-like distance measure between the "fog aware" statistics of the test image and the MVG models obtained from the natural foggy and fog-free images, respectively.

To evaluate the performance of the proposed model, a subjective study is performed using another 100 foggy image set consisting of newly recorded foggy images, well-known standard defog test images, and the corresponding defogged output images. Results demonstrate that the predicted perceptual fog density of the proposed model correlates well with human judgments of fog density on a variety of foggy images.

The remainder of this paper is organized as follows. Section 2 summarizes the optical model of foggy image formation and characteristics of foggy images. The perceptual fog density prediction model is described in Section 3. We then explain the executed human subjective study in Section 4 and evaluate the performance of the proposed model in Section 5. We conclude this paper with future work in Section 6.

2. OPTICAL FOGGY IMAGE FORMATION AND CHARACTERISTIS

2.1 Optical foggy image formation

Although the accurate nature of scattering is complex due to diverse particles constituting a media and characteristics of the incident light[2], the simplified Koschmieder's atmospheric scattering model[14] has been used to explain optical foggy image formation.[5-13] When light from the sun passes through a scattering fog atmosphere, light reflected from objects is directly attenuated along the path to the camera. Moreover, light scattered by the atmosphere, which is called "airlight," is added to the camera and makes the scene color shifted. Mathematically, the captured image of a foggy scene I is represented as the linear combination of direct attenuation and airlight as follows.

$$I(x) = J(x)t(x) + A\left[1 - t(x)\right], \tag{1}$$

where $J(x)$ is the scene radiance or a fog-free image at each pixel x, $t(x) \in [0,1]$ is the transmission of the reflected light in the atmosphere, and A is the global atmospheric skylight that represents ambient light in the atmosphere. By assuming the atmosphere is homogenous, and by considering the light traveling a longer distance is more attenuated and scattered, the transmission $t(x)$ is expressed as $t(x) = \exp[-\beta d(x)]$, where β is a medium attenuation coefficient, and $d(x)$ is scene depth from the camera at pixel position x.

2.2 Characteristics of foggy images

The simplified Koschmieder's atmospheric scattering model explains observable characteristics of foggy images such as low contrast, faint color, and shifted intensity.[5, 13] When we measure the contrasts of an image as the magnitude of its gradient field or edge (or the number of edges), a scene radiance $J(x)$ seen through a homogenous medium in iso-depth regions with $t(x) = t < 1$ can be described as

$$\left\| \nabla I(x) \right\| = \left\| t\nabla J\left(x\right) + (1-t)\nabla A \right\| = \left\| t\nabla J(x) \right\| < \left\| \nabla J(x) \right\|, \tag{2}$$

where $\| \nabla \cdot \|$ indicates the number of pixels whose gradients are larger than a given threshold. Hence, the contrast of foggy scenes is lower than that of fog-free scenes. In addition, since every pixel at each *RGB* color channel has the same depth, the color of a foggy image is fainter than that of a fog-free image as depth increases from a camera to scene objects. This can be explained as

$$\lim_{d\to\infty} \frac{\left| I_i(x) - I_j(x) \right|}{\left| J_i(x) - J_j(x) \right|} \approx \lim_{d\to\infty} e^{-\beta d(x)} = 0, \tag{3}$$

where $|\cdot|$ denotes an absolute value and $i, j \in \{r, g, b\}$ represents *RGB* channels.

Furthermore, since the global atmospheric skylight A is larger than the intensity of I, the intensity of foggy scenes is larger than that of fog-free scenes as below:

$$A - I(x) = \left[A - J(x) \right] t(x) > 0,$$
$$I(x) - J(x) = \left[A - J(x) \right] \left[1 - t(x) \right] > 0, \tag{4}$$

3. PERCEPTUAL FOG DENSITY PREDICTION MODEL

The proposed perceptual fog density prediction model is based on the extraction of fog aware statistical features and fitting them to a multivariate Gaussian (MVG)[21] model. The fog aware statistical features are derived using a space domain regular natural scene statistic (NSS)[15, 16] model and observed characteristics of foggy images described in Section 2. A test foggy image is applied to compute a Mahalanobis-like distance between the MVG fit of the fog aware statistical features obtained from the test image and the MVG model of the fog aware features extracted from a corpus of 160 foggy images and fog-free images, respectively. Each corresponding distance is defined as a foggy level and a fog-free level. The perceptual fog density is then expressed as the ratio of the foggy level to the fog-free level of the test image.

3.1 Fog aware statistical features

The first and the second fog aware statistical features are derived from local image patches. The essential low order statistics of foggy and fog-free images, which are perceptually relevant, are derived from a spatial domain NSS model of local mean subtracted contrast normalized coefficients (MSCN)[16]. Ruderman observed that such normalized luminance values strongly tend towards a unit normal Gaussian characteristic on good quality photographic images.[15] In addition, divisive normalization is related to the contrast-gain masking process in early human vision.[22, 23] For natural foggy images, we have found that the variance of the MSCN coefficients increases as fog density increases. Furthermore, the variance of the pairwise product of neighboring MSCN coefficients along the vertical orientation exhibits a regular structure. Hence, we use both as fog aware statistical features and compute them as follows:

$$I_{MSCN}(i,j) = \frac{I_{gray}(i,j) - \mu(i,j)}{\sigma(i,j) + 1}, \tag{5}$$

$$\mu(i,j) = \sum_{k=-K}^{K} \sum_{l=-L}^{L} \omega_{k,l} I_{gray}(i+k, j+l), \tag{6}$$

$$\sigma(i,j) = \sqrt{\sum_{k=-K}^{K} \sum_{l=-L}^{L} \omega_{k,l} [I_{gray}(i+k, j+l) - \mu(i,j)]^2}, \tag{7}$$

$$I_{Vpair\_MSCN}(i,j) = I_{MSCN}(i,j) \cdot I_{MSCN}(i+1, j), \tag{8}$$

where $i \in \{1, 2, \ldots, M\}$, $j \in \{1, 2, \ldots, N\}$ are spatial indices, M and N are the image dimensions, and $\omega = \{\omega_{k,l} | k = -K, \ldots, K, l = -L, \ldots, L\}$ is a 2D circularly symmetric Gaussian weighting function sampled out to 3 standard deviations ($K = L = 3$) and rescaled to unit volume,[16] and I_{gray} is the grayscale version of I.

Other fog aware statistical features are derived from observed characteristics of foggy images including low contrast, faint color, and shifted intensity by using the local mean and the coefficient of variance for sharpness,[17] the Michelson contrast[18], the image entropy[19], the pixel-wise dark channel prior[9], the color saturation in *HSV* color space, and the colorfulness[20]. Since the standard deviation, $\sigma(i, j)$, is a key factor of structural image information to capture and quantify local image sharpness[17], and the impact of $\sigma(i, j)$ can be different according to the center value, $\mu(i, j)$, we compute the coefficient of variation,

$$\xi(i,j) = \frac{\sigma(i,j)}{\mu(i,j)}, \tag{9}$$

to measure the normalized dispersion of probability distribution, and use both $\sigma(i, j)$ and $\xi(i, j)$ as fog aware features.

The Michelson contrast (MC) measures the relation between the spread and the sum of luminances that take up similar fractions of an area.[18] It is useful to determine the relative visibility of scene radiance to scattered airlight introduced into the view path by fog obscuring the scene behind it. It is expressed as

$$MC(i,j) = \frac{I_{\max} - I_{\min}}{I_{\max} + I_{\min}}, \tag{10}$$

where $I_{\max}$ and $I_{\min}$ are maximum and minimum values at each 2×2 pixel window, respectively. Since two single points of extreme brightness or darkness can determine the measure of contrast of the whole image, we used the smallest window (2×2 pixels) size to capture a local contrast.

Entropy is a measure of uncertainty of a random variable.[19] The entropy of an image (*IE*) describes the amount of detail information. For example, an image having lower entropy (e.g., a blue sky) contains very little variations and large runs of pixels with the same or similar values, while an image having higher entropy (e.g., a forest with colorful trees) includes richer details. Since foggy images contain less amount of detail information, we use *IE* as a fog aware feature and compute it as follows,

$$IE(I) = -\sum_{\forall i} p(h_i) \log\left[p(h_i) \right], \tag{11}$$

where $p(h_i)$ is the probability of the pixel intensity h_i, which is estimated from the normalized histogram.

The dark channel prior is based on the observation on outdoor haze-free images: in most non-sky or haze-free regions, at least one color channel has some pixels whose intensity are very low and close to zero. Equivalently, the minimum intensity in such a region is close to zero.[8] We use a pixel-wise model of the dark channel prior[9],

$$I_{dark}(i,j) = \min_{c \in \{r,g,b\}} \left[I_c(i,j) \right], \tag{12}$$

where $c \in \{r, g, b\}$ represents *RGB* channels. We normalize the intensity of I_{dark} from zero to one. Regions of high value in I_{dark} indicate sky, fog, or white object regions. Conversely, regions of low value in I_{dark} represent fog-free regions.

To measure the visibility of a foggy scene with regards to color vision, we use the color saturation and the colorfulness as fog aware features. Since airlight scattered in a foggy atmosphere can cause scene color shifts, for denser foggy scenes, the color saturation and the colorfulness decrease. The color saturation, $I_{saturation}$, is represented by a saturation channel after a foggy image is transformed into *HSV* color space by using a MATLAB function "rgb2hsv," while the colorfulness (CF) indicating a perceptual variety and intensity of colors is computed as follows[20],

$$I_{saturation}(i,j) = I_{HSV}(i,j,2), \tag{13}$$

$$CF = \sqrt{\sigma_{rg}^2 + \sigma_{yb}^2} + 0.3\sqrt{\mu_{rg}^2 + \mu_{yb}^2}, \tag{14}$$

$$\sigma_a^2 = \frac{1}{X} \sum_{x=1}^{X} (a_x^2 - \mu_a^2), \tag{15}$$

$$\mu_a = \frac{1}{X} \sum_{x=1}^{X} a_x, \tag{16}$$

where I_{HSV} is a transformed image of I into *HSV* color space, $rg = R - G$, and $yb = 0.5(R + G) - B$.[24] The pixel values of an image came from the range $x = 1 \ldots X$. Table 1 summarizes a total of 9 local fog aware statistical features.

Table 1. A summary of "fog aware" statistical features.

Feature ID	Feature Description	Computation
f_1	The variance of MSCN coefficients	(5)
f_2	The variance of the vertical product of MSCN coefficients	(8)
f_3	The sharpness	(7)
f_4	The coefficient of variance of sharpness	(9)
f_5	The Michelson contrast	(10)
f_6	The image entropy	(11)
f_7	The dark channel prior in a pixel-wise	(12)
f_8	The color saturation in *HSV* color space	(13)
f_9	The colorfulness	(14)

3.2 Patch selection

A total of 9 local fog aware statistical features are computed from each $P \times P$ partitioned image patch. To obtain fog aware statistical features for each patch, we use the average value of each computed $f_3 \sim f_5$, f_7, and f_8 at each patch, while we directly calculate f_1, f_2, f_6, and f_9 for each patch. For a collection of fog aware statistical features from a corpus of 160 natural foggy and fog-free images, respectively, only a subset of the patches are used. Since humans tend to evaluate the visibility of foggy images based on regions of high sharpness, contrast, and saliency, and since every image is subject to some kind of limiting distortions including defocus blur,[25] we use only a subset of the image patches, while, for a test foggy image, all patches are used.

We select representative image patches that include rich information of the fog aware statistical features. Let the $P \times P$ sized patches be indexed $b = 1, 2 \ldots B$. First, the average feature value of each patch indexed b at feature number m is computed as

$$\delta_m(b) = \frac{1}{P^2} \sum_{i=1}^{P} \sum_{j=1}^{P} f_m(i, j), \tag{17}$$

where $f_m(i, j)$ denotes feature coefficients at feature number m, (m = 1, 3, 5, 6, 7, and 8). Second, to obtain patches from a corpus of natural fog-free images, we select the average feature value having $\delta_m > T_m$ (when m = 7, $\delta_m < T_m$). The threshold, T_m is chosen to be a fraction q_m of the peak patch feature value over the image except when m = 7. In our experiments, q_m = 0.7 when m = 1, 3, 5, 6, and 8, and T_7 = 0.4. We have observed small differences in performance when q_m is varied in the range [0.6 0.8] and T_7 is varied in [0.3 0.5]. Similarly, to obtain patches from a corpus of natural foggy images, we execute the same process with an opposite inequality sign (i.e., " > "). All of the parameters described here are tested in a wide range of patch sizes from 4 × 4 to 160 × 160 pixels. The patch size can be decided variously, and the image patches can be overlapped to any desired degree, with fog density prediction performance generally rising with greater overlap. An example of patch selection is shown in Figure 1.

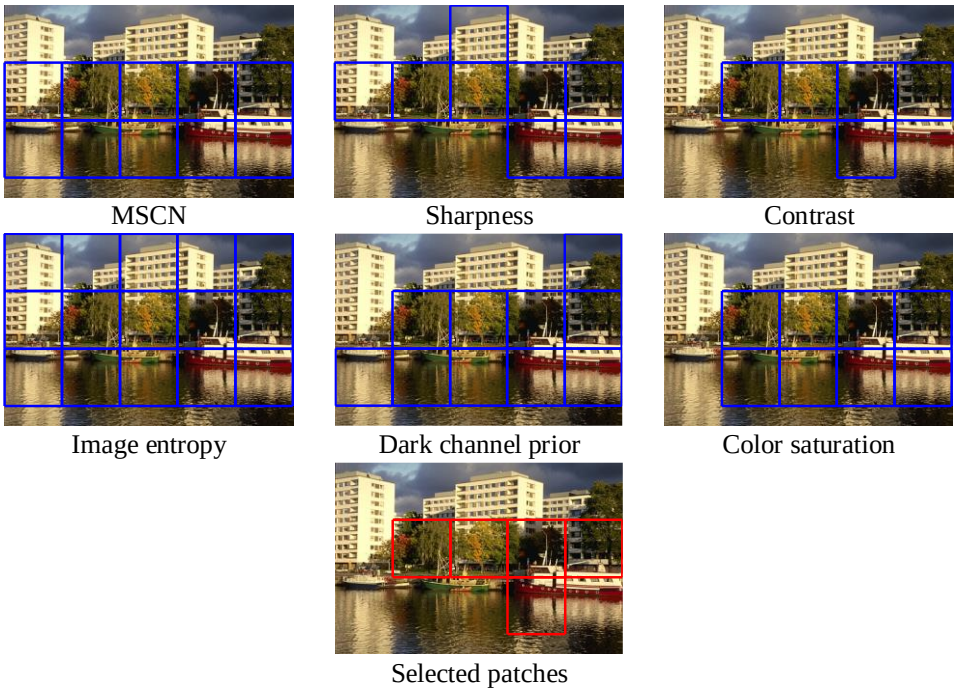

Figure. 1. A patch selection procedure using local fog aware statistical features. The blue marked patches in the first two rows show the satisfied patches for each feature selection criterion. The red marked patches in the third row represent the finally selected patches. A patch size is 96 × 96 pixels, and an image size is 480 × 320 pixels, respectively.

3.3 Natural fog-free and foggy image data sets

To extract fog aware statistical features from a corpus of fog-free images, we selected a wide-ranging set of 160 natural fog-free images from the LIVE IQA database[26], the Berkeley image segmentation database[27], and the CSIQ image database[28]. Image sizes vary from 480 × 320 to 768 × 512 pixels, and fog-free images are selected to have highly diverse contents. Some sample images are displayed in Figure 2.

Figure. 2. Sample images of a corpus of 160 natural fog-free images.

Similarly, to extract fog aware statistical features from a corpus of foggy images, we selected a wide-ranging set of 160 natural foggy images from a copy-right free website data, newly recorded foggy images, and well-known defog test images[5-13]. Image sizes vary from 380 × 234 to 950 × 564 pixels. Some sample images are displayed in Figure 3.

Figure. 3. Sample images of a corpus of 160 natural foggy images.

3.4 Perceptual fog density prediction

A test foggy image is partitioned into $P \times P$ patches. All patches are then used to compute the average feature values to yield a set of 9 fog aware statistical features at each patch. Next, the foggy level, D_f, of a test foggy image is computed as a Mahalanobis-like distance between a multivariate Gaussian (MVG)[21] fit of fog aware statistical features extracted from the test foggy image and a MVG model of the fog aware features extracted from a corpus of 160 natural fog-free images. The general MVG density in d dimensions is

$$MVG(\boldsymbol{f}) = \frac{1}{(2\pi)^{d/2}|\boldsymbol{\Sigma}|^{1/2}} \exp\left[-\frac{1}{2}(\boldsymbol{f}-\boldsymbol{v})^t \boldsymbol{\Sigma}^{-1}(\boldsymbol{f}-\boldsymbol{v})\right] \tag{18}$$

where $\boldsymbol{f}$ is the set of fog aware statistical features computed as in (1) ~ (16), and $\boldsymbol{v}$ and $\boldsymbol{\Sigma}$ denote the mean and d-by-d covariance matrix, and $|\boldsymbol{\Sigma}|$ and $\boldsymbol{\Sigma}^{-1}$ are the determinant and inverse, respectively, of the covariance matrix under the MVG model, which are estimated using a standard maximum likelihood estimation procedure[21] as follows:

$$\boldsymbol{v} = \mathcal{E}[\boldsymbol{f}], \tag{19}$$

$$\boldsymbol{\Sigma} = \mathcal{E}\left[(\boldsymbol{f}-\boldsymbol{v})(\boldsymbol{f}-\boldsymbol{v})^t\right], \tag{20}$$

where $\mathcal{E}[\cdot]$ denotes the expected value, and t indicates transpose. The Mahalanobis-like distance is computed as

$$D_f(\boldsymbol{v}_1, \boldsymbol{v}_2, \boldsymbol{\Sigma}_1, \boldsymbol{\Sigma}_2) = \sqrt{(\boldsymbol{v}_1-\boldsymbol{v}_2)^t \left(\frac{\boldsymbol{\Sigma}_1+\boldsymbol{\Sigma}_2}{2}\right)^{-1} (\boldsymbol{v}_1-\boldsymbol{v}_2)}, \tag{21}$$

where $\boldsymbol{v}_1$, $\boldsymbol{v}_2$ and $\boldsymbol{\Sigma}_1$, $\boldsymbol{\Sigma}_2$ are the mean vectors and covariance matrices of the MVG model in a fog-free corpus and the MVG fit of a test foggy image, respectively. Similarly, the fog-free level, D_{ff}, of a test foggy image is also computed as a distance between a MVG fit of fog aware statistical features extracted from the test foggy image and an MVG model from a corpus of 160 foggy images. Finally, the perceptual fog density, D, of a foggy image is achieved as follows,

$$D = \frac{D_f}{D_{ff}+1}, \tag{22}$$

where a constant "1" is used to prevent a denominator from being a zero. Smaller value of D indicates lower perceptual fog density. Figure 4 shows an overall block diagram of the proposed perceptual fog density prediction model.

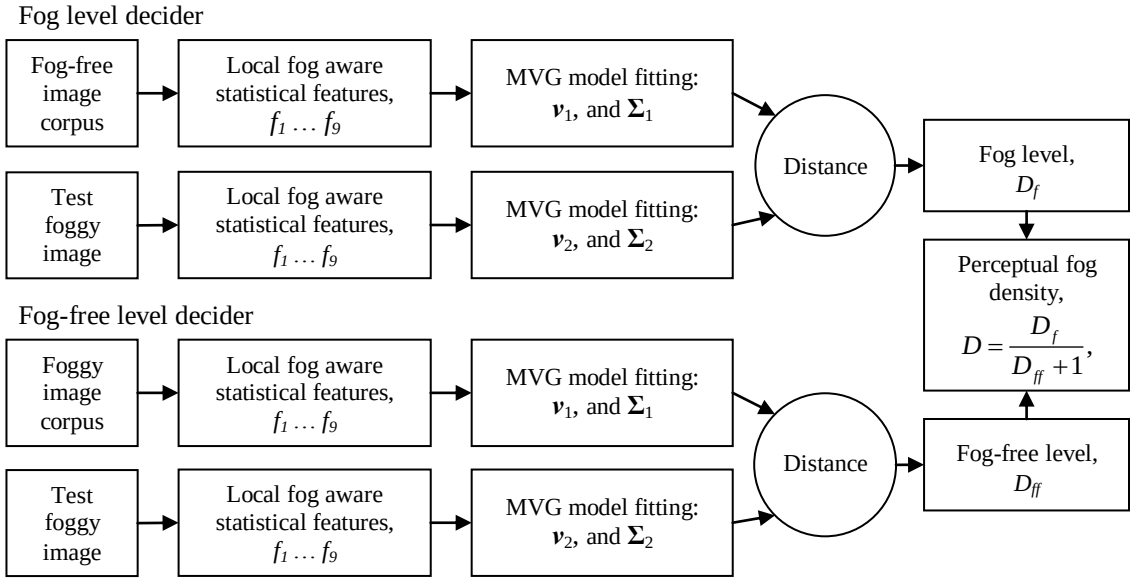

Figure. 4. Block diagram of the proposed perceptual fog density prediction model.

4. HUMAN SUBJECTIVE STUDY

4.1 Test image set

To test the performance of the proposed perceptual fog density prediction model, a human subjective study was performed using another 100 test images consisting of newly recorded foggy images, well-known defog test images[5-13], and the corresponding defogged output images. Image sizes varied from 425 × 274 to 1024 × 768 pixels. Some sample images are displayed in Figure 5.

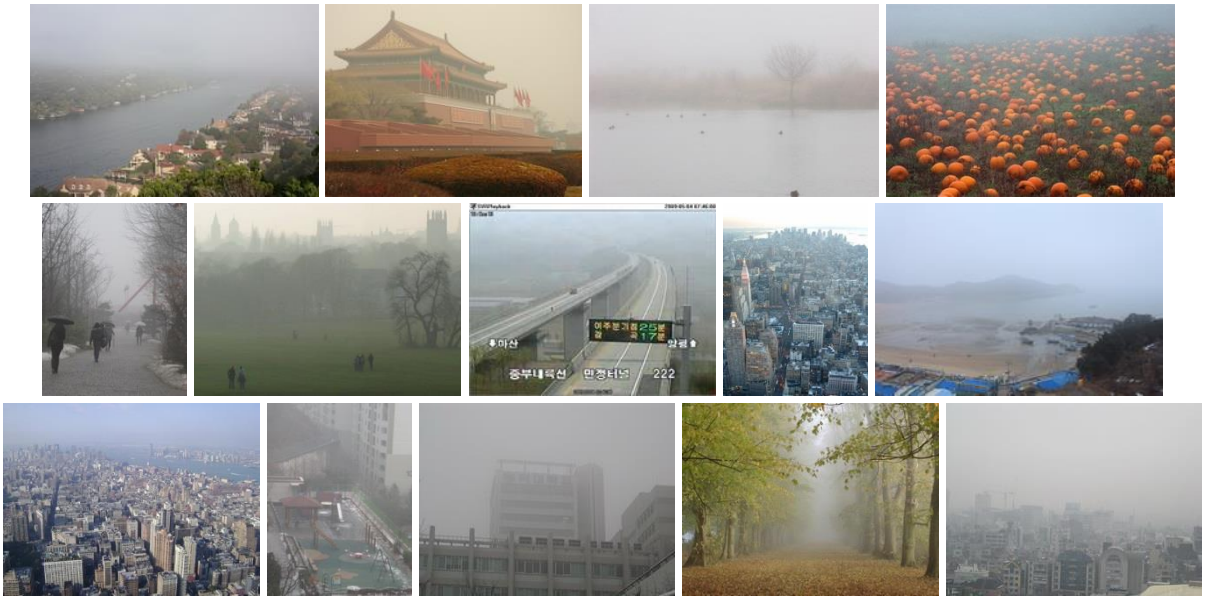

Figure. 5. Sample images from the 100 test image set used in a human subjective study.

4.2 Methodology

A total of 20 naïve students at The University of Texas at Austin rated the fog density of images using a single-stimulus continuous quality evaluation (SSCQE)[29] method. All subjects were between the ages of 20 and 35. No vision test was performed although a verbal confirmation of soundness of (corrected) vision was obtained from the subjects. Each subject attended one session that lasted less than 30 minutes, which consisted of the subject viewing 100 randomized test images. A short training set (10 images) preceded the actual study.

The test images were displayed on the center of the 15" LCD monitor (Dell, Round Rock, TX, USA) at a resolution of 1920 × 1080 pixels for 8 seconds by using a specially designed MATLAB program and the Psychophysics toolbox[30]. The subjects were requested to rate the fog density of the test images at the end of each display. A continuous bar calibrated as "Hardly", "Little", "Medium", "Highly", and "Extremely" by markings, equally spaced across the bar, was displayed on the center of the screen, where "Highly" corresponded to "I think the test image contains high fog density." The fog density ratings were in the range from 0 to 100, where 0 means fog-free. Once the judgment was received using a mouse, the subject was not allowed to change the score. There was no rejected subject in the subject screening procedure[29], so all of the subjective study data was used for the evaluation of the proposed model.

5. RESULTS

The proposed model not only predicts perceptual fog density for an entire image but also provides a local perceptual fog density prediction for each patch size. Figure 6 shows the results of the proposed model over non-overlapped diverse patch sizes from 4 × 4 to 160 × 160 pixels, where the predicted fog density is shown visually in gray scales ranging from black (low) to white (high). Results using a smaller patch size yield a more detailed fog density map.

Test foggy image

4 × 4

8 × 8

10 × 10

16 × 16

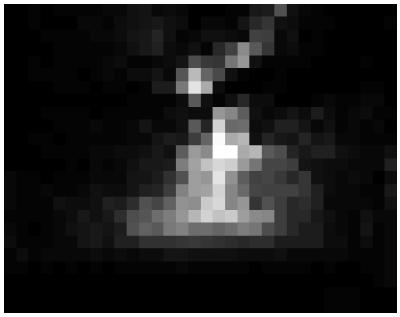

32 × 32

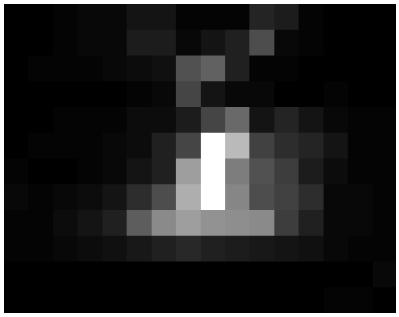

64 × 64

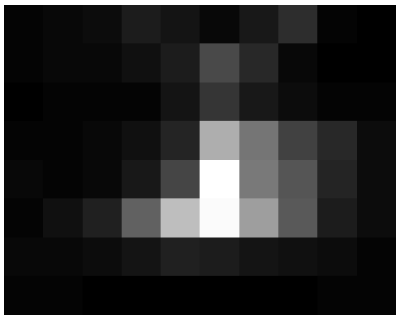

96 × 96

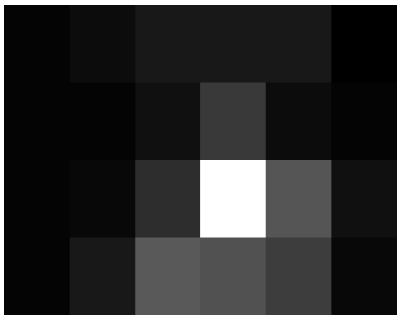

160 × 160

Perceptual fog density

Figure. 6. The results of the proposed perceptual fog density prediction model over diverse patch sizes from 4 × 4 to 160 × 160 pixels. The predicted perceptual fog density is shown visually by gray levels ranging from black (low) to white (high).

To evaluate the performance of the proposed model, we utilized Pearson's linear correlation coefficient (LCC) and Spearman's rank ordered correlation coefficient (SROCC). The predicted perceptual fog density scores of the proposed model were passed through a logistic non-linearity[26] before computing LCC and SROCC relative to fog density scores on foggy images from the human subjects. The logistic function[26] is

$$logisitc(y) = \beta_1 \left\{ 0.5 - \frac{1}{1+\exp\left[\beta_2 (y - \beta_3)\right]} \right\} + \beta_4 y + \beta_5, \tag{23}$$

where y is the predicted fog density score produced by the proposed model, and $\beta_1 \ldots \beta_5$ are parameters which are estimated through a non-linear curve fitting procedure[26]. The performance of the proposed model was compared using diverse patch sizes ranging from 4 × 4 to 160 × 160 pixels. The LCC and SROCC of the proposed model for a patch size 8 by 8 is 0.8748 and 0.8578, respectively, while the LCC and SROCC across a wide range of patch sizes show stable performance over all test fog images as shown in Table 2.

Table 2. The performance of the proposed model on 100 test images: the predicted perceptual fog density of the proposed model and the mean of all subject's measured fog density on 100 test images were evaluated using Pearson's linear correlation coefficient (LCC) and Spearman's rank ordered correlation coefficient (SROCC) over diverse patch sizes.

Patch size	4 × 4	8 × 8	10 × 10	16 × 16	32 × 32	64 × 64	96 × 96	160 × 160
LCC	0.8732	**0.8748**	0.8740	0.8713	0.8602	0.8536	0.8444	0.8150
SROCC	**0.8618**	0.8578	0.8575	0.8597	0.8515	0.8502	0.8386	0.7875

In addition, we validated the possibility of the proposed model as a tool to assess the performance of defog algorithms by comparing the predicted fog density of defogged images with the corresponding measured fog density from the human subjects. The high correlation between the predicted fog density of the proposed model and the measured fog density from human judgments indicates that the proposed model can reasonably evaluate the performance of defog algorithms. Table 3 tabulates LCC and SROCC of the predicted fog density scores after a logistic non-linearity[26] against human subjective scores for two defog test image sets shown in Figure 7. Although the results present a potential possibility of the proposed model as a visibility assessment tool, since only a small number of image sets were tested, for better validation, a subjective study using a larger number of foggy and defogged image test sets is planned.

Table 3. The performance of the proposed model as a tool to assess defog algorithms on 10 test images shown in Figure 7. The predicted perceptual fog density of the proposed model and the mean of all subject's measured fog density were evaluated by using Pearson's linear correlation coefficient (LCC) and Spearman's rank ordered correlation coefficient (SROCC) over diverse patch sizes.

Patch size	4 × 4	8 × 8	10 × 10	16 × 16	32 × 32	64 × 64	96 × 96	160 × 160
LCC	0.9348	0.9381	0.9417	0.9444	0.9532	**0.9652**	0.9573	0.9628
SROCC	0.5758	0.6606	0.6606	0.6606	0.6364	**0.7939**	0.7818	0.7697

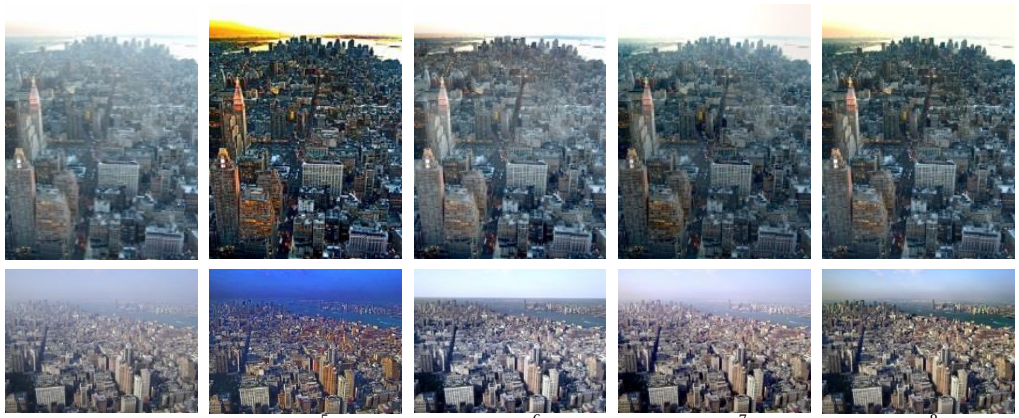

Foggy image Tan[5] Koph[6] Fattal[7] He[8]

Figure. 7. The original foggy images and the corresponding defogged images[5-8] used in a subjective study.

6. CONCLUSION AND FUTURE WORK

We have proposed a perceptual fog density prediction model that estimates the degree of visibility of a foggy scene from a single image using "fog aware" statistical features. The features that define the perceptual fog density are obtained from a corpus of natural foggy and fog-free images based on a spatial domain natural scene statistics (NSS) model and observed characteristics of foggy images. The perceptual fog density is expressed as the ratio of the foggy level to the fog-free level of a test foggy image, where the foggy level and the fog-free level are computed using a Mahalanobis-like distance between the MVG fit of the fog aware statistical features of the test image and the MVG models obtained from the natural foggy and fog-free images, respectively. The predicted perceptual fog density correlates well with human judgments of fog density when applied to 100 test images. We have also found that the proposed fog density prediction model can be used as a visibility assessment tool on the results of defog algorithms. The proposed model may be improved by adding more perceptually relevant fog aware statistical features into a current framework. Future work would involve creating a perceptual defog algorithm to enhance the visibility of foggy scenes based on the proposed perceptual fog density prediction model. In addition, for better validation of the proposed model as a visibility assessment tool, we plan to execute a human subjective study with a larger number of foggy image data sets.

ACKNOWLEDGMENTS

This work (Grants No. C0014365) was supported by Business for Cooperative R&D between Industry, Academy, and Research Institute funded Korea Small and Medium Business Administration in 2013.

REFERENCES

[1] Nayar, S. K., and Narasimhan, S. G., "Vision in Bad Weather," *Proceedings of the Seventh IEEE International Conference on Computer Vision*, 820-827 (1999).
[2] Narasimhan, S. G., and Nayar, S. K., "Contrast restoration of weather degraded images," *IEEE Transactions on Pattern Analysis and Machine Intelligence*, 25(6), 713-724 (2003).
[3] Pomerleau, D., "Visibility estimation from a moving vehicle using the RALPH vision system," *Proceedings of the IEEE Intelligent Transportation System*, 906-911 (1997).
[4] Hautière, N., Tarel, J. -P., Lavenant, J., and Aubert, D., "Automatic fog detection and estimation of visibility distance through use of an onboard camera," *Machine Vision and Applications*, 17(1), 8-20 (2006).
[5] Tan, R. T., "Visibility in bad weather from a single image," *Proceedings of the IEEE Conference on Computer Vision and Pattern Recognition*, 1-8 (2008).
[6] Kopf, J., Neubert, B., Chen, B., Cohen, M., Cohen-Or, D., Deussen, O., Uyttendaele, M., and Lischinski, D., "Deep photo: Model-based photograph enhancement and viewing," *ACM Transactions on Graphics*, 27(5), 116:1-116:10 (2008).
[7] Fattal, R., "Single image dehazing," *ACM Transactions on Graphics, SIGGRAPH*, 27(3), 72 (2008).
[8] He, K., Sun, J., and Tang, X., "Single image haze removal using dark channel prior," *Proceedings of the IEEE Conference on Computer Vision and Pattern Recognition*, 1956-1963 (2009).
[9] Ancuti, C., Hermans, C., and Bekaert, P., "A fast semi-inverse approach to detect and remove the haze from a single image," *Proceedings of the 10th Asian Conference on Computer Vision*, 501-514 (2010).
[10] Tarel, J. -P., and Hautière, N., "Fast visibility restoration from a single color or gray level image," *Proceedings of the IEEE 12th International Conference on Computer Vision*, 2201-2208 (2009).
[11] Hautière, N., Tarel, J. -P., Aubert, D., and Dumont, E., "Blind contrast enhancement assessment by gradient ratioing at visible edges," *Image Analysis and Stereology Journal*, 27(2), 87-95 (2008).
[12] Yu J., and Liao, Q., "Fast single image fog removal using edge-preserving smoothing," *Proceedings of the IEEE International Conference on Acoustics, Speech and Signal Processing*, 1245-1248 (2011).
[13] Qi, B., Wu, T., and He, H., "A new defogging method with nested windows," *Proceedings of the IEEE International Conference on Information Engineering Computer Sciences*, 1-4 (2009).
[14] Koschmieder, H., "Theorie der horizontalen sichtweite," in *Beitrage zur Physik der Freien Atmosphare*. Munich, Germany: Keim & Nemnich, (1924).
[15] Ruderman, D. L., "The statistics of natural images," *Network: Computataion in Neural Systems*, 5(4), 517-548 (1994).

[16] Mittal, A., Moorthy, A. K., and Bovik, A. C., "No-reference image quality assessment in the spatial domain," *IEEE Transactions on Image Processing*, 21(12), 4695-4708 (2012).
[17] Mittal, A., Soundararajan, R., and Bovik, A. C., "Making a completely blind image quality analyzer," *IEEE Signal Processing Letters*, 20(3), 209-212 (2013).
[18] Michelson, A. A., [Studies in Optics], University of Chicago Press, (1927).
[19] Shannon, C. E., "A mathematical theory of communication," *Bell System Technical Journal*, 27, 379 -423 (1948).
[20] Hasler, D., and Susstrunk, S., "Measuring colourfulness in natural images," *Proceedings of the SPIE Human Vision and Electronic Imaging*, 5007, 87-95 (2003).
[21] Duda, R. O., and Hart, P. E., and Stork, D. G., [Pattern classification]. Wiley-Interscience, (2012).
[22] Carandini, M., Heeger, D. J., and Movshon, J. A., "Linearity and normalization in simple cells of the macaque primary visual cortex," *The Journal of Neuroscience*, 17(21), 8621-8644 (1997).
[23] Wainwright, M. J., Schwartz, O., and Simoncelli, E. P., "Natural image statistics and divisive normalization: Modeling nonlinearities and adaptation in cortical neurons," in *Statistical Theories of the Brain*. Cambridge, MA: MIT Press, 203-222 (2002).
[24] Winkler, S., "Analysis of public image and video databases for quality assessment," *IEEE Journal of Selected Topics in Signal Processing*, 6(6), 616-625 (2012).
[25] Bovik, A. C., "Perceptual image processing: Seeing the future," *Proceedings of the IEEE*, 98(11), 1799-1803 (2010).
[26] Sheikh, H. R., Sabir, M. F., and Bovik, A. C., "A statistical evaluation of recent full reference image quality assessment algorithms," *IEEE Transactions on Image Processing*, 15(11), 3440-3451 (2006).
[27] Martin, D. Fowlkes, C., Tal, D., and Malik, J., "A database of human segmented natural images and its application to evaluating segmentation algorithms and measuring ecological statistics," *Proceedings of the Eighth IEEE International Conference on Computer Vision*, 416-423 (2001).
[28] Larson, E. C., and Chandler, D. M., "Full-reference image quality assessment and the role of strategy," *Journal of Electronic Imaging*, 19(1), 011006 (2010).
[29] ITU-R BT.500-11, "Methodology for the subjective assessment of the quality of television pictures," International Telecommunication Union Standardization, (2002).
[30] Brainard, D. H., "The psychophysics toolbox," *Spatial Vision*, 4(4), 433-436 (1997).